analytical chemistry

Article

Cite This: *Anal. Chem.* 2018, 90, 10144−10151

pubs.acs.org/ac

Frequency Shift Raman-Based Sensing of Serum MicroRNAs for Early Diagnosis and Discrimination of Primary Liver Cancers

Wen-Feng Zhu,[†] Lin-Xiu Cheng,[†,‡,⊥] Min Li,[*,†] Duo Zuo,[§] Ning Zhang,[§] Hong-Jun Zhuang,[†] Dan Xie,[†] Qing-Dao Zeng,[‡] James A. Hutchison,[*,∥] and Yu-Liang Zhao[*,†,‡]

[†]CAS Key Laboratory for Biomedical Effects of Nanomaterials and Nanosafety, Institute of High Energy Physics, Chinese Academy of Sciences, 19B Yuquan Road, Shijingshan District, Beijing 100049, China

[‡]CAS Key Laboratory of Standardization and Measurement for Nanotechnology, CAS Center for Excellence in Nanoscience, National Center for Nanoscience and Technology, No. 11 Beiyitiao, Zhongguancun, Beijing 100190, China

[§]Department of Cancer Cell Biology, Tianjin Medical University Cancer Institute and Hospital, National Clinical Research Center for Cancer, Key Laboratory of Cancer Prevention and Therapy, Tianjin's Clinical Research Center for Cancer, Tianjin 300060, China

[∥]School of Chemistry and Bio21 Institute, University of Melbourne, 30 Flemington Road, Parkville Victoria 3052 Australia

[⊥]University of the Chinese Academy of Sciences, 19A Yuquan Road, Shijingshan District, Beijing 100049, P. R. China

Supporting Information

ABSTRACT: Frequency shift surface-enhanced Raman scattering (SERS) achieves multiplex microRNA sensing for early serological diagnosis of, and discrimination between, primary liver cancers in a patient cohort for whom only biopsy is effective clinically. Raman reporters microprinted on plasmonic substrates shift their vibrational frequencies upon biomarker binding with a dynamic range allowing direct, multiplex assay of serum microRNAs and the current best protein biomarker, α-fetoprotein. Benchmarking against current gold-standard polymerase chain reaction and chemiluminescence methods validates the assay. The work further establishes the frequency shift approach, sensing shifts in an intense SERS band, as a viable alternative to conventional SERS sensing which involves the more difficult task of resolving a peak above noise at ultralow analyte concentrations.

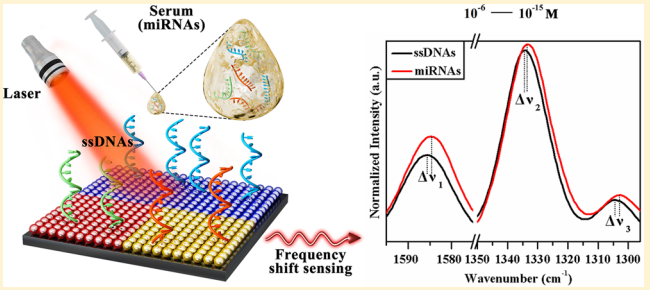

Liver cancer kills >700 000 people every year with near-unity mortality-to-incidence ratio.[1] Incidence is low but rising in western countries and concentrated in East Asia with over half of the cases occurring in China.[2] Liver cancer is the primary cause of cancer-related deaths for East Asians of working age (<60 years), and the median age of sufferers in a high incidence region in China is 48, the prime of working life.[3,4] The terrible human cost is thus accompanied by productivity losses in a region critical to global GDP growth but now challenged by aging demographics, making liver cancer both an important health and economic issue of our time.[5,6]

Around 85% of primary liver cancers (PLCs) are hepatocellular carcinomas (HCC), associated with hepatitis B/C infection or aflatoxin exposure in developing countries, and alcohol-related cirrhosis or fatty liver disease in the West.[3,7,8] The remaining 15% involve intrahepatic cholangiocarcinomas (ICC) of the biliary duct, often associated with chronic inflammation due to parasitic liver fluke infestation.[9,10] For example, ICC is the dominant PLC in Issan populations in northeast Thailand where as many as 70% of the population can carry the *opisthorchis viverrini* parasite due to dietary preference for under-cooked fish.[9] The 5 year survival rate for PLCs is ∼10%.[3]

This poor prognosis is due in large part to late onset of symptoms, often too late for current viable curative treatments, surgical resection, or transplant. Even if detected early when targeted intervention is crucial, morphological discrimination between a few millimeters diameter HCC and ICC tumors is not trivial.[10] Current best serum biomarkers, such as α-fetoprotein (AFP) for HCC, suffer from low sensitivity and selectivity in early disease stages.[11] Improving methods for early detection and discrimination of PLCs remains thus a matter of urgency.

Recently it was established that dysregulation of specific combinations of circulating microRNAs (miRNAs) can be diagnostic of early stage PLC and a predictor of disease stage and prognosis.[11,12] However, the typical pico-to-femtomolar serum concentrations of miRNAs, and their homologous structures, makes their quantification challenging. Quantitative,

Received: April 22, 2018
Accepted: July 5, 2018
Published: July 5, 2018

DOI: 10.1021/acs.analchem.8b01798
Anal. Chem. 2018, 90, 10144−10151

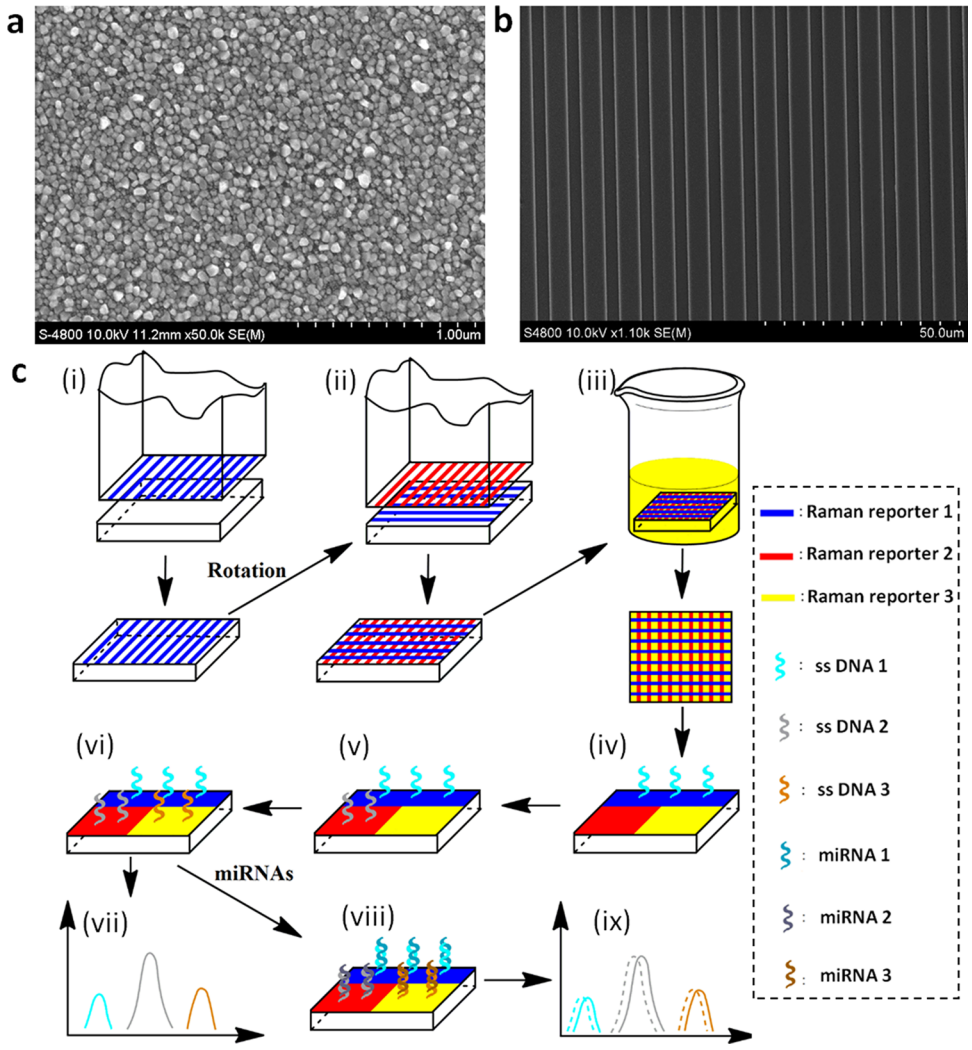

Figure 1. SERS frequency shift method for multiplex microRNA sensing: (a) scanning electron microscope (SEM) image of the silver nanoparticle film (AgNF) substrates; (b) SEM image of the patterned PDMS film for stamping; and (c) schematic of chemisorption of aromatic thiol Raman reporters to the AgNFs surface (i–iii), coupling ssDNA to the reporters (iv–vi), miRNAs capture and SERS frequency shift readout (vii–ix).

real-time-polymerase chain reaction (qRT-PCR) is the current gold standard amplification method but suffers from the lack of house-keeping genes in serum for normalization.[13] Competing techniques include Northern analysis, microarray, electrochemical, fluorometry, and many others.[14−18] Enhanced optical fields due to coupled surface plasmon resonances (SPR) at nanogaps between metallic nanoparticles may allow direct miRNA detection (without amplification), either by measuring shifts in the SPR energy due to refractive index changes upon miRNA binding or via surface-enhanced Raman scattering (SERS).[19]

The recently introduced SERS frequency shift method, in which a normal mode vibrational frequency of a Raman reporter is shifted upon analyte binding, combines the strengths of the latter two SPR sensing modalities.[20−25] It retains the excellent multiplexing capability of SERS, with multiple analytes being identifiable by their spectral fingerprint in a single read-out. Meanwhile, like refractive index methods, it requires measurement of a shift in an intense signal rather than resolving a peak above noise, easing spectroscopic resolution requirements.

Here a SERS frequency shift method is developed for three important challenges in the sphere of PLC diagnostics: multiplex serum miRNA quantification for diagnosis of early stage HCC; the simultaneous quantification of serum miRNA and α-fetoprotein in HCC sufferers; and the quantification of serum miRNA for discrimination between HCC and ICC. In each case, the method is applied to serum from groups of 5−10 patients from the Tianjin Medical University Cancer Institute and Hospital, China, and compared to healthy controls where relevant. The results are validated against current best methods for serum microRNA and protein quantification, qRT-PCR, and electrochemiluminescence, respectively, showing excellent agreement.

EXPERIMENTAL SECTION

A full account of the materials and methods employed is included in the Supporting Information. Silver nanoparticle films used as SERS substrates were prepared by a modified Tollen's method.[25] Domains of aromatic thiol Raman reporters were chemisorbed to the AgNFs by microcontact printing followed by conjugation of antisense DNA or antibody for capture of miRNAs and AFP, respectively. SERS spectra were recorded on a DXR Smart Raman spectrometer (Thermo Fisher, 633 or 780 nm, 80 mW, 10 μm diameter laser focal spot, 15 s integration time, room temperature). The substrates

DOI: 10.1021/acs.analchem.8b01798
Anal. Chem. 2018, 90, 10144−10151

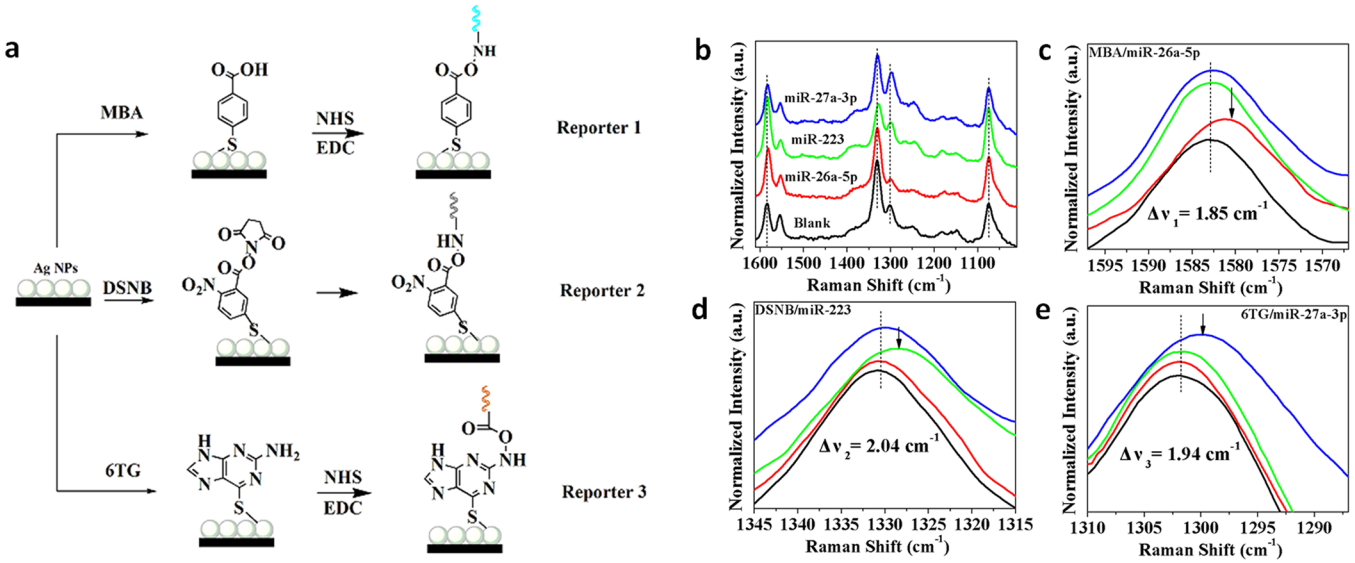

Figure 2. Raman reporter vibrational frequency shifts after hybridization with miRNA. (a) Schematic of the chemical structure of the aromatic thiols bound to the AgNFs to give MBA-derived reporter 1, DSNB-derived reporter 2, and 6TG-derived reporter 3. (b) SERS spectra of the AgNFs substrate modified by reporters 1−3 after exposure to saline-sodium citrate (SSC) buffered aqueous solutions (black curve) and to SSC solutions containing only miR-26a-5p (miRNA 1, red curve), only miR-223 (miRNA 2, green curve), and only miR-27a-3p (miRNA 3, blue curve) in micromolar concentrations. Spectra are offset on the intensity scale for ease of comparison; (c−e) the same SERS spectra expanded to show the 1585 cm^{-1} peak due to MBA-derived reporter 1, the 1334 cm^{-1} peak due to DSNB-derived reporter 2, and 1301 cm^{-1} peak due to 6TG-derived reporter 3, respectively.

were kept immersed in either 3× saline-sodium citrate (SSC) buffer or fetal bovine serum (FBS) during irradiation. Standard curves for Raman frequency shift were developed using known solutions of synthetic miRNAs and recombinant AFP in FBS. Serum samples from Tianjin Medical University Cancer Institute were kept at −20 °C for storage and defrosted to 4 °C before use. The 100 μL serum samples were diluted with 900 μL of FBS and 20 units of RNase inhibitor added to prevent miRNA degradation, then substrate binding/SERS measurements were undertaken exactly as for the standard curves.

RESULTS AND DISCUSSION

SERS Frequency Shift Methodology. The SERS frequency shift method for multiplex detection of PLC-associated miRNAs herein begins with synthesis of silver nanoparticle films (AgNFs) with ~10^7 enhancement factors for SERS (Figure 1a, see the Supporting Information for full experimental details). Mercaptobenzoic acid (MBA), 5,5′-dithiobis(succinimidyl-2-nitrobenzoate (DSNB), and 6-thioguanine (6TG) were employed as Raman reporters, each having thiol or disulfide bonds for chemisorption to AgNFs, a high scattering cross-section for a vibration in an uncluttered spectral region for shift-sensing (see Figure S-1) and activated carboxylic coupling functionality for binding to single strand DNA (ssDNA) for miRNA capture. MBA and DSNB were chemisorbed to the AgNFs in arrays of 3 μm-width lines oriented perpendicularly by polydimethylsiloxane (PDMS) microcontact printing (Figure 1b,c). 6TG was chemisorbed to the remaining bare regions by soaking. ssDNA complementary to each targeted miRNA was sequentially linked to the surface bound aromatics giving Raman reporters 1−3, respectively (Figure 2a). Laser excitation over a 10 μm diameter spot overlaps each reporter domain, and resulting SERS spectra show strong bands at 1585 cm^{-1} due to aromatic C−C stretches of MBA-derived reporter 1, at 1334 cm^{-1} due to the nitro stretch of DSNB-derived reporter 2, and at 1301 cm^{-1} due to the ring C−N stretches of 6TG-derived reporter 3 (Figure 2b). Hybridization of target miRNAs to the ssDNA induces shifts to lower frequency in these bands, constituting the assay. Exposing the substrate to saline−sodium citrate solutions containing only one miRNA causes frequency shifts only in the vibrational mode of the reporter with complementary ssDNA attached (Figure 2c−e). Other bands such as the 1075 cm^{-1} C−S stretch are unaffected within the uncertainty of the measurement (*vide infra*, Figure 2b and Supporting Information, Figure S-2).

Batch-to-Batch Reproducibility of Raman Response. The reproducibility of Raman signals from plasmonic substrates is a common issue for SERS-based sensing methods. We assessed the SERS signal intensity for the 1585 cm^{-1} band of an MBA monolayer chemisorbed to our AgNFs at the 633 and 780 nm excitation wavelengths used in this study. The monolayer was prepared by soaking the AgNF in a 10^{-3} M MBA/ethanol solution followed by rinsing with SSC buffer. SERS spectra were then taken with the substrate immersed in fetal bovine serum (FBS). SERS signals were recorded at three randomly selected positions on each substrate for 5 parallel substrates prepared from 3 different batches. The SERS response was highly uniform with relative standard deviations less than 8% and 3% for 633 and 780 nm laser excitation respectively (Supporting Information, Figure S-3). The reproducibility of the frequency shifts observed upon miRNA binding was also assessed for the 1585 cm^{-1} band of a MBA monolayer chemisorbed to an AgNF. The MBA was bound to ssDNA complementary to the microRNA miR-26a-5p for these measurements (see next section and Materials and Methods in the Supporting Information). The change in Raman shift of the ~1585 cm^{-1} band was measured after incubating the substrate with miR-26a-5p in FBS in concentrations ranging from 10^{-6} to 10^{-16} M (Supporting

DOI: 10.1021/acs.analchem.8b01798
Anal. Chem. 2018, 90, 10144−10151

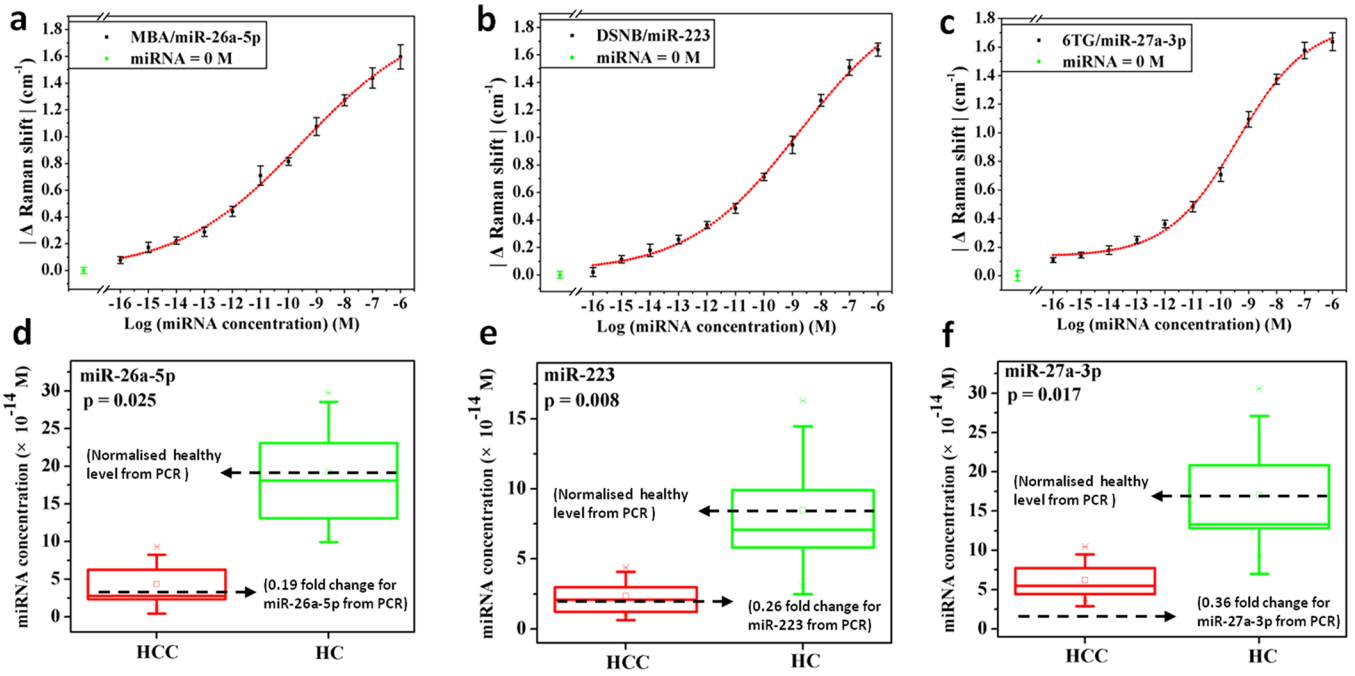

Figure 3. SERS frequency shift multiplex assay of miRNAs in human serum. (a–c) Absolute change in Raman shift (|ΔRaman shift|) of reporter 1–3, respectively, upon exposing a AgNF substrate modified with all three reporters to FBS solutions equimolar in synthetic miR-26a-5p, miR-223, and miR-27a-3p. (d–f) Simultaneous SERS frequency shift assay of serum miR-26a-5p, miR-223, and miR-27a-3p concentrations, respectively, for early stage HCC sufferers (BCLC stage 0–A, n = 10) and healthy controls (HC, n = 10). Box plots (median/interquartile range, whisker length one standard deviation), mean value (open square), and extreme values (crosses) are indicated. Dashed lines indicate the relative change in miRNA expression measured in serum from a similar cohort (BCLC stage 0–A, n = 55) by qRT-PCR (ref 11).

Information, Figure S-4). Substrates from 7 and 3 different batches were studied with laser excitation at 633 and 780 nm. The average standard deviation in the measured shifts across this concentration range, across substrates, and using 633 and 780 nm excitation was 0.04 cm^{-1}. The standard deviation of repeated measurements of the peak Raman shift on the same sample and same position was 0.03 cm^{-1}, slightly higher than the value of 0.022 cm^{-1} given in an application note for the DXR Raman spectrometer used herein.[26] The measured uncertainty in frequency shift is consistent with the uncertainties in the two measurements required to calculate it adding in quadrature, suggesting the errors are random and uncorrelated. Defining the limit of detection (LOD) for the sensor as 3 times this uncertainty gives a value of 0.12 cm^{-1} as the minimum measurable shift. Again, we note that the measurement of a shift in an intense Raman band, which depends mainly on the precision of the instrument, avoids the onerous task of resolving a peak above noise at ultralow analyte concentrations.

Multiplex microRNA Sensor Performance. Serum levels of microRNAs miR-26a-5p, miR-223, and miR-27a-3p were targeted for multiplex sensing as they have been shown to be dysregulated in HCC patient serum by other methods.[11,12] Substrates discussed above with microcontact-printed regions of the three Raman reporters bound with ssDNA complementary for these miRNAs were employed.

First, standard curves were developed for the absolute change in Raman shift (|ΔRaman shift|) at the 1585 cm^{-1} aromatic C–C stretch of MBA-derived reporter 1, at the 1334 cm^{-1} nitro stretch of DSNB-derived reporter 2, and at the 1301 cm^{-1} ring C–N stretch of 6TG-derived reporter 3, respectively, upon exposure of the substrate to FBS solutions equimolar in synthetic miR-26a-5p, miR-223, and miR-27a-3p, in the range 10^{-6} to 10^{-16} M. The experiments were repeated 6 times on 2 different samples, and the average |ΔRaman shift| as a function of concentration is plotted in Figure 3a–c. The plots have a sigmoidal form as semilog plots and were fit to Boltzmann functions by nonlinear least-squares fitting to produce standard curves for sensing unknown samples. The reference value for the frequency shifts was measured in exactly the same way but with exposure of the substrate to FBS solution without any synthetic miRNAs (green points in Figure 3a–c).

We note that standard curves developed in SSC buffer were very similar suggesting that nonspecific binding by proteins in FBS was minimal. The shifts in the three Raman reporter bands induced by a solution of the three synthetic miRNAs at 10^{-15} M are shown in detail in Figure 4. As seen in the insets of Figure 4, the raw data is collected with points every 0.5 cm^{-1}. Peak maxima are extracted following b-spline interpolation or fitting the peaks to voigt functions and the peak maximum are quoted to a final precision of 0.01 cm^{-1}. All three miRNAs cause shifts above 0.11 cm^{-1} at 10^{-15} M concentration with an average shift of 0.14 cm^{-1}, and thus 10^{-15} M is estimated to be the LOD. For miRNAs solution concentrations of the order of 10^{-15} M, given incubating solution volumes of 1 mL, a sample area of 0.8 × 0.9 cm^2 stamped with probes, and that 1/3 of the 10 μm excitation spot area contains one kind of probe, there would be ~10 of each miRNA in the excitation spot assuming complete binding.

Specificity of the Multiplex microRNA Sensor. Nonspecific binding can degrade sensor performance. As a proof-of-principle test of the specificity of the multiplex sensing of miR-26a-5p, miR-223, and miR-27a-3p, SSC buffer solutions of synthetic versions of all 3 miRNAs were spiked with 200 ng/mL glypican 3 (GPC3). GPC3 is a heparan sulfate

DOI: 10.1021/acs.analchem.8b01798
Anal. Chem. 2018, 90, 10144–10151

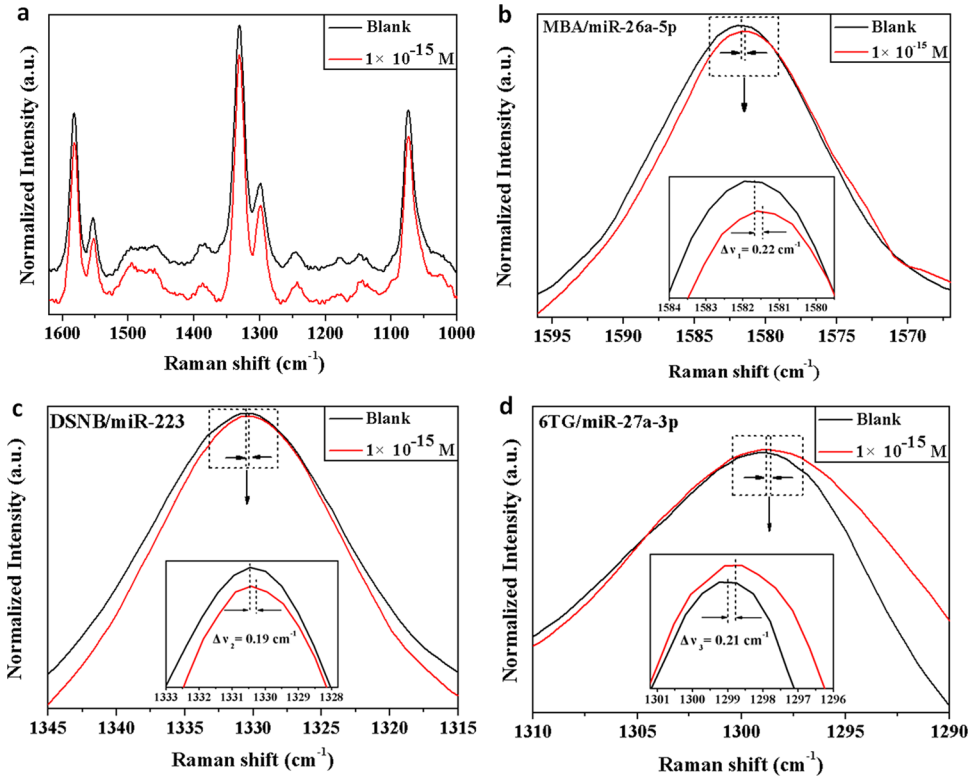

Figure 4. Frequency shifts at the limit of detection for multiplex miRNA detection. (a) SERS spectra of the AgNF substrate modified with reporters 1−3 upon exposure to FBS solutions without (black curve) and with (red curve) 10^{-15} M synthetic miR-26a-5p, miR-223, and miR-27a-3p. (b) The same spectra expanded in the region around 1580 cm^{-1} where the aromatic C−C stretch of MBA-derived reporter 1 is down-shifted by interaction with miR-26a-5p. (c) The same spectra expanded in the region around 1334 cm^{-1} where the nitro stretch of DSNB-derived reporter 2 is down-shifted by interaction with miR-223. (d) The same spectra expanded in the region around 1301 cm^{-1} where the purine C−N stretch of the 6TG-derived reporter 3 is down-shifted by interaction with miR-27a-3p. Insets show the peak regions in more detail.

proteoglycan that is elevated to 10−100 ng/mL (>10^{-10} M) levels in HCC patients.[27] The frequency shifts in the Raman reporters measured in the presence and absence of GPC3 were the same within uncertainty for a range of synthetic miRNAs concentrations down to the LOD (Supporting Information, Figure S-5).

Vibrational Frequency Shift Mechanism. The excellent sensitivity and selectivity of the assay is attributed to the drastic restructuring of the reporter-bound ssDNA monolayer upon miRNAs hybridization, affecting the vibrational frequencies of multiple reporters in the vicinity of a binding event.[28−30] Hybridization of similar length ssDNA monolayers is known to induce large (>10 nm) increases in height and expulsion of structural water, with concomitant softening and order-of-magnitude reduction in the Young's modulus of the layer.[31,32] The resulting reporter vibrational frequency shifts to lower energy observed herein could thus be due to mechanical stretching (reduction in stiffness) of the relevant bonds induced by structural change in the ssDNA overlayer. However, changes in reporter solvation dielectric constant (vibrational Stark effect, VSE) or specific hydrogen bonding effects due to local dehydration could also contribute.[29,33]

To test the latter hypothesis, the Raman reporter vibrational frequencies of interest for shift-sensing were measured in solvents of wide ranging static dielectric constant and hydrogen bonding ability to assess whether the observed frequency shifts could indeed be associated with solvation changes upon miRNAs hybridization with the antisense ssDNA-bound Raman reporter. The nitro group of substrate-bound DSNB shows a strong red-shift with solvent polarity in aprotic solvents, similar to that observed for the stretch of other polar groups such as nitriles and attributed to VSE (Supporting Information, Figure S-6).[29,33] A blue-shift is observed in water, attributed to hydrogen bonding interactions, again similar to the behavior of nitrile stretches.[29,33] However, both the purine C−N stretch of 6TG and aromatic C−C stretch of MBA show relatively weak solvent dependencies (±1 cm^{-1} relative to toluene). Therefore, it is likely that mechanical deformations account for the frequency shifts observed herein; however, the relative contributions of the various mechanisms discussed above will be the subject of further work.

Multiplex microRNA Sensing in Preclinical HCC Patient Serum. The frequency shift assay was tested on serum from a patient cohort presenting at the Tianjin Medical University Cancer Institute and Hospital in late 2016 who tested positive for hepatitis B surface antigen and exhibited focal liver lesions during imaging. Lesion morphology and serum protein biomarkers cannot definitively establish disease etiology in such cohorts. Early stage HCC (stage 0−A on the Barcelona Clinic Liver Cancer (BCLC) scale) was diagnosed in part of the cohort only after biopsy and histology. Serum from 10 of these patients was compared to serum from 10 healthy controls (HC) using the frequency shift method for multiplex sensing of miR-26a-5p, miR-223, and miR-27a-3p (patient gender and age details for this and all studies are included in the Supporting Information, Table S-1). All participants throughout this study gave informed consent in writing and the study was approved by the ethical committee

DOI: 10.1021/acs.analchem.8b01798
Anal. Chem. 2018, 90, 10144−10151

of the Tianjin Medical University Cancer Institute and Hospital. Assay operators were blind to serum identity.

Inclusion criteria for patients diagnosed with stage 0−A HCC were patients with chronic hepatitis B (positive for hepatitis B surface antigen for at least 6 months prior to the start of the study), >18 years of age, no previous history of any cancer, and no infection with other hepatic viruses. Inclusion criteria for the healthy controls were no evidence of infectious or malignant liver disease or positive makers for hepatic viruses in the preceding 5 years as assessed during annual health examinations, >18 years.

The results of the multiplex assay showed that mean serum concentration was significantly different (p value < 0.03) and lower in the HCC patient group compared to the healthy control group (HC) for all three miRNAs (Figure 3d−f and Table 1). The relative expression of these miRNAs in a similar cohort of preclinical HCC patients presenting at the same medical center between 2012−2014 and healthy controls (HC), as determined by qRT-PCR, were in excellent agreement especially for miR-26a-5p and miR-223 (Figure 3d−f and Table 1).[11] The aforementioned issue with normalization during amplification means that PCR can provide accurate relative change in miRNA concentration between patient cohort and healthy controls, which can be compared with the absolute miRNA concentrations that are assayed by our SERS frequency shift method.

Table 1. Multiplex microRNA Quantification for Early Diagnosis of HCC[a]

	mean expression ($\times 10^{-14}$ M)		expression ratio: HC/HCC	
miRNA	HCC (n = 10)	HC (n = 10)	frequency shift SERS	qRT-PCR[b]
miR-26a-5p	4.33 ± 2.60	19.23 ± 6.21	4.30	5.30
miR-223	2.35 ± 1.15	8.47 ± 3.99	3.60	3.80
miR-27a-3p	6.18 ± 2.19	17.03 ± 6.69	2.80	9.10

[a]Simultaneous SERS frequency shift assay of serum miR-26a-5p, miR-223, and miR-27a-3p concentrations for early stage HCC sufferers (BCLC stage 0-A, n = 10) and healthy controls (n = 10), samples collected at Tianjin Medical University Cancer Institute and Hospital, late 2016. The healthy/HCC expression ratio is compared to that determined by qRT-PCR for a similar cohort (samples collected at Tianjin Medical University Cancer Institute and Hospital, 2012-2014, BCLC stage 0-A, n = 55, from ref 11. [b]Data from ref 11.

Simultaneous Protein and microRNA Sensing in HCC Patient Serum. Serum concentration of α-fetoprotein is the best-established noninvasive test for liver cancer in current practice.[34,35] Despite its shortcomings in sensitivity and selectivity, the large database existing for the relationship between AFP and liver cancer may assist in understanding microRNA relationships to liver cancer. The combination of polytype serum biomarkers such as miRNAs and AFP may be especially important for diagnosis and clinical surveillance of HCC given the genetic variation in individual cases and resulting varying expression of biomarkers.[35−37] Thus, the assay was modified to detect miR-26a-5p and miR-223 simultaneously with AFP using the same methodology as described above but coupling AFP antibodies to the 6TG-coated regions of the sensor substrate. As there are several orders of magnitude difference between typical miRNAs and AFP expression levels in human serum, standard curves were produced for the simultaneous sensing of miR-26a-5p and miR-223 in the range 10^{-11} to 10^{-16} M and for AFP in the range 3.6×10^{-7} to 3.6×10^{-12} M in FBS (Supporting Information, Figure S-7).

The polytype sensor was used to simultaneously assay miR-26a-5p, miR-223, and AFP in serum from 5 patients with HCC at various stages (BCLC stage A−C, double blind measurements, see also Table S-1 for gender and age details). The assayed concentrations of miRNAs and AFP for each patient are included in Table S-2 and shown in Figure 5a,b. Serum concentrations of AFP and the miRNAs are anticorrelated for the sample set, suggesting that useful relationships between miR-26a-5p and miR-223 and AFP may exist (Figure 5a).[11] A correlation between biomarker concentration and disease stage is however less clear in this small cohort (Table S-2) and this will be assessed with extended studies in the future. Importantly, the AFP expression levels in the sera tested were also determined by electrochemiluminescent immunoassay (ECLIA), a standard clinical technology, showing excellent agreement with the results of the SERS frequency shift assay (Figure 5b and Table S-2).

Discrimination between HCC and ICC. Discrimination between the main forms of PLCs, HCC and ICC, expedites targeted response, particularly aiding tumor location for

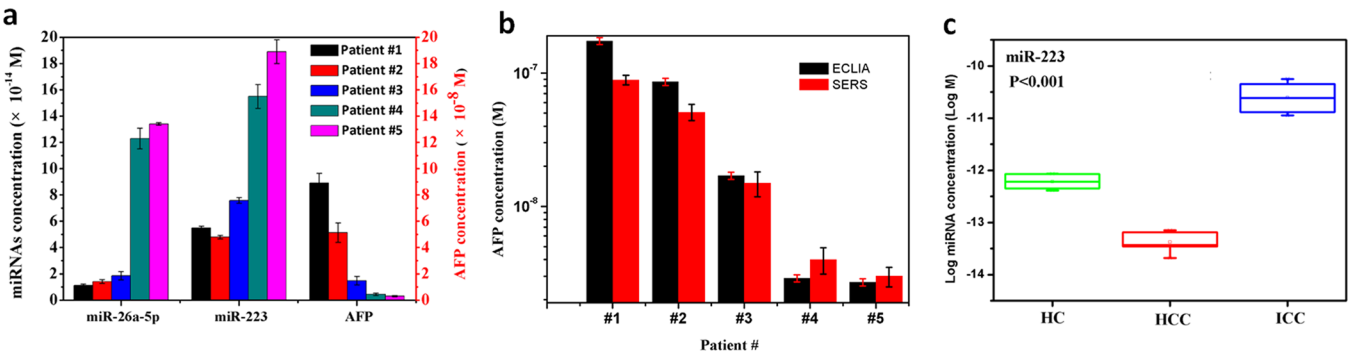

Figure 5. Simultaneous microRNA and protein sensing and HCC/ICC discrimination. (a) Simultaneous SERS frequency shift assay of serum miR-26a-5p, miR-223, and α-fetoprotein (AFP) for 5 HCC sufferers (BCLC stage A-C). (b) Comparison of serum AFP concentrations measured by electrochemiluminescence (ECLIA) and SERS frequency shift assay for the 5 HCC sufferers; error bars are 1 standard deviation. (c) SERS frequency-shift assay of serum miR-223 concentration for 6 HCC (BCLC stage B-C) and 5 ICC sufferers (TMN stage II-IV), and 5 healthy controls (HC), box plots (median/interquartile range, whisker length one standard deviation) with mean value (open square) and extreme values (crosses) are indicated.

DOI: 10.1021/acs.analchem.8b01798
Anal. Chem. 2018, 90, 10144−10151

imaging or resection.[9,10] MiRNA-223 is known to be down-regulated for HCC and up-regulated for ICC in qRT-PCR studies.[37] Therefore, patterned substrates with just two domains for anti-AFP-bound MBA, and the ssDNA-bound DSNB-derived reporter, were utilized to simultaneously detect AFP and miRNA-223 (see Materials and Methods in the Supporting Information).

Standard curves were developed in FBS solutions containing AFP at 10^{-8}−10^{-13} M and synthetic miRNA-223 at 10^{-11}−10^{-16} M concentration ranges respectively (Supporting Information, Figure S-8). Again, both the MBA-derived aromatic C−C breathing modes and the DSNB-derived nitro stretch frequencies shift to lower frequencies upon binding AFP and miRNA-223, respectively. The standard curves show that the response to miRNA-223 is more sensitive in this configuration as compared with the case for sensing 3 miRNAs simultaneously (Figure 3b) and the semilog plots could be fit with linear functions (Supporting Information, Figure S-8). For the sensing of three miRNAs simultaneously, DSNB-derived monolayers were microcontact printed onto substrates. For HCC/ICC discrimination, DNSB-derived monolayers were chemisorbed to bare substrate areas by soaking. The latter case likely gives a more perfect monolayer, accounting for the increased sensitivity.

Simultaneous SERS frequency shift assay of serum concentrations of miRNA-223 and AFP were undertaken for 6 patients with HCC (stage B-C, BCLC), 5 healthy controls (HC), and 5 patients with ICC (stage II-IV, TNM classification) and the results shown in Figure 5c and collected in the Supporting Information, Table S-3. The inclusion criteria for ICC patients were patients identified to have ICC by biopsy/histology and staged according to the TNM classification, >18 years of age, and with no other history of cancer.

The frequency shift assay reveals excellent differentiability ($p < 0.001$) between the 3 patient groups (Figure 5c). Specifically, the serum concentrations of miRNA-223 were found to be up-regulated for the ICC patients (10^{-11} M) and down-regulated for the HCC patients ($10^{-15} \sim 10^{-14}$ M), compared to the HC (10^{-13} M) (see also the Supporting Information, Table S-3). Once again the concentration of AFP determined by the frequency shift method agreed well with the same measurement made by ECLIA (Table S-3). Examples of SERS spectra taken after incubation with sera from an ICC patient, an HCC patient, and a healthy control are included in the Supporting Information, Figure S-8.

This work suggests that the SERS frequency shift method combined with microcontact printing as applied to direct, multiplex detection of serum microRNA and protein biomarkers has the potential to become a highly flexible and effective tool for primary liver cancer diagnostics in clinical settings. The great strength of the technique is its combination of picomolar sensitivity for direct assay of serum miRNA with a dynamic range allowing simultaneous assay of established protein biomarkers at nanomolar or greater concentrations. While the sample sizes studied are small in this proof-of-principle study, the assay results compares very well with gold-standard methods for serum microRNA and protein detection, qRT-PCR, and electrochemiluminescent assay.

From a methodological viewpoint, several improvements could be made to enhance the clinical utility of the assay. As sharp vibrational bands are employed (~20 cm^{-1} width) there is genuine scope for improvement in the multiplexing capability of the assay beyond the three miRNAs/proteins developed herein. This would require more sophisticated microcontact printing of the substrate and selection of Raman reporters with appropriate functional groups for coupling and with vibrational modes that do not overlap those employed currently for shift sensing. Assaying larger suites of microRNA or protein biomarkers would enhance the specificity of the assay for PLC diagnostics and prognostics.

Using the methodology described herein, assay results are available 24 h after patient serum is obtained. Most of this time is devoted to the soaking/binding stage and could be reduced to less than a day by using less dilution of serum samples. This short time frame could make the assay a genuine frontline screening option for at-risk patients, (e.g., those presenting with chronic hepatitis B and liver lesions) and preclude in some cases the need for biopsy and immunohistochemical analysis. The disadvantages associated with the latter are well-known and include its invasive nature, the possibility of inducing tumor metastasis during tissue extraction, variable diagnoses depending on the location of the slice taken and handler experience, cost, and the time required (typically at least 5 days).

CONCLUSION

As already mentioned, current gold-standard microRNA sensing by polymerase chain reaction methods has issues with absolute quantification of circulating microRNAs.[13] This work suggests that the SERS frequency shift method combined with microcontact printing is a genuine candidate among others in development[14−18] to offer a cheaper, less cumbersome, and more accurate approach to multiplex assaying of serum microRNAs for the early detection and discrimination of primary liver cancers. Further work is required, however, with the current priority being a larger scale trial of the frequency shift assay at the Tianjin Medical University Cancer Institute and Hospital with a view to establishing it alongside currently accepted technologies for diagnosis of preclinical HCC. Additional future efforts will be directed toward a more robust assessment of PLC staging and prognosis via longitudinal studies using the frequency shift assay.

ASSOCIATED CONTENT

Supporting Information

The Supporting Information is available free of charge on the ACS Publications website at DOI: 10.1021/acs.analchem.8b01798.

Experimental section, SERS spectra of the aromatic thiol Raman reporters, insensitivity of Raman reporter C−S stretch to miRNA, batch-to-batch reproducibility of Raman shift and intensity, interference from other tumor-specific biomarkers, solvent dependence of reporter Raman bands, patient inclusion criteria, staging, consent, gender and age, simultaneous sensing of miRNA and AFP for HCC patients, and discrimination between HCC and ICC (PDF)

AUTHOR INFORMATION

Corresponding Authors

*E-mail: limin@ihep.ac.cn.
*E-mail: James.hutchison@unimelb.edu.au.
*E-mail: zhaoyuliang@ihep.ac.cn.

DOI: 10.1021/acs.analchem.8b01798
Anal. Chem. 2018, 90, 10144−10151

ORCID

Min Li: 0000-0003-2959-9080
Qing-Dao Zeng: 0000-0003-3394-2232
Yu-Liang Zhao: 0000-0002-9586-9360

Author Contributions

M.L. conceived the multiplex liver cancer biomarker detection strategy based on the SERS frequency shift. J.A.H. and M.L. elucidated the frequency shift mechanism. W.-F.Z. implemented the 3 miRNAs multiplex assay experiments, the 2 miRNAs + AFP assay experiments, the batch-to-batch reproducibility experiments, the interference experiments, the solvent dependence experiments, and participated in data analysis. L.-X.C. performed the HCC/ICC discrimination measurements and participated in data analysis. D.Z. and N.Z. provided the serum samples and valuable discussion on microRNA. W.-F.Z., M. L., and J.A.H. wrote the manuscript. M.L., J.A.H., and Y.-L.Z. supervised the project. All authors discussed the results and commented on the manuscript at all stages.

Notes

The authors declare no competing financial interest.

■ ACKNOWLEDGMENTS

This work was supported by the National Natural Science Foundation of China (Grant No. 31671012), the National Basic Research Program of China (Grant No. 2015CB932004), and the Australian Research Council DECRA scheme (Grant DE130101300).

■ REFERENCES

(1) Ferlay, J.; Soerjomataram, I.; Dikshit, R.; Eser, S.; Mathers, C.; Rebelo, M.; Parkin, D. M.; Forman, D.; Bray, F. *Int. J. Cancer* **2015**, *136*, E359−E386.

(2) Bertuccio, P.; Turati, F.; Carioli, G.; Rodriguez, T.; Vecchia, C.; Malvezzi, M.; Negri, E. *J. Hepatol.* **2017**, *67*, 302−309.

(3) Chen, W.; Zheng, R.; Baade, P. D.; Zhang, S.; Zeng, H.; Bray, F.; Jemal, A.; Yu, X. Q.; He. *Ca-Cancer J. Clin.* **2016**, *66*, 115−132.

(4) Zhong, J.; Peng, N.-F.; You, X.-M.; Ma, L.; Xiang, X.; Wang, Y.-Y.; Gong, W.-F.; Wu, F.-X.; Xiang, B.-D.; Li, L.-Q. *Oncotarget* **2017**, *8*, 18296−18302.

(5) Chung, W. *Clin. Mol. Hepatol.* **2015**, *21*, 14−21.

(6) Salgado, R. *Regional Economic Outlook, April 2017, Asia and Pacific: Preparing for Choppy Seas*, International Monetary Fund: Washington, DC, 2017.

(7) Petrick, J. L.; Braunlin, M.; Laversanne, M.; Valery, P. C.; Bray, F.; McGlynn, K. A. *Int. J. Cancer* **2016**, *139*, 1534−1545.

(8) Llovet, J. M.; Zucman-Rossi, J.; Pikarsky, E.; Sangro, B.; Schwartz, M.; Sherman, M.; Gores, G. *Nat. Rev. Dis. Primers* **2016**, *2*, 16018.

(9) Liengswangwong, U.; Nitta, T.; Kashiwagi, H.; Kikukawa, H.; Kawamoto, T.; Todoroki, T.; Uchida, K.; Khuhaprema, T.; Karalak, A.; Srivatanakul, P.; Miwa, M. *Int. J. Cancer* **2003**, *107*, 375−380.

(10) Zhou, X. D.; Tang, Z.-Y.; Fan, J.; Zhou, J.; Wu, Z.-Q.; Qin, L.-X.; Ma, Z.-C.; Sun, H.-C.; Qiu, S.-J.; Yu, Y.; Ren, N.; Ye, Q.-H.; Wang, L.; Ye, S.-L. *J. Cancer Res. Clin. Oncol.* **2009**, *135*, 1073−1080.

(11) Zuo, D.; Chen, L.; Liu, X.; Wang, X.; Xi, Q.; Luo, Y.; Zhang, N.; Guo, H. *Tumor Biol.* **2016**, *37*, 6539−6549.

(12) Zhou, J.; Yu, L.; Gao, X.; Hu, J.; Wang, J.; Dai, Z.; Wang, J.-F.; Zhang, Z.; Lu, S.; Huang, X.; Wang, Z.; Qiu, S.; Wang, X.; Yang, G.; Sun, H.; Tang, Z.; Wu, Y.; Zhu, H.; Fan, J. *J. Clin. Oncol.* **2011**, *29*, 4781−4788.

(13) Marabita, F.; de Candia, P.; Torri, A.; Tegnér, J.; Abrignani, S.; Rossi, R. L. *Briefings Bioinf.* **2016**, *17*, 204−212.

(14) Lanford, R. E.; Hildebrandt-Eriksen, E. S.; Petri, A.; Persson, R.; Lindow, M.; Munk, M. E.; Kauppinen, S.; Ørum, H. *Science* **2010**, *327*, 198−201.

(15) Szczyrba, J.; Löprich, E.; Wach, S.; Jung, V.; Unteregger, G.; Barth, S.; Grobholz, R.; Wieland, W.; Stöhr, R.; Hartmann, A.; et al. *Mol. Cancer Res.* **2010**, *8*, 529−538.

(16) Ren, Y.; Deng, H.; Shen, W.; Gao, Z. *Anal. Chem.* **2013**, *85*, 4784−4789.

(17) Hong, C. Y.; Chen, X.; Li, J.; Chen, J.-H.; Chen, G.; Yang, H.-H. *Chem. Commun.* **2014**, *50*, 3292−3295.

(18) Tian, T.; Wang, J.; Zhou, X. *Org. Biomol. Chem.* **2015**, *13*, 2226−2238.

(19) Hill, R. T. *WIREs Nanomed. Nanobiotechnol.* **2015**, *7*, 152−168.

(20) Guerrini, L.; Pazos, E.; Penas, C.; Vázquez, M. E.; Mascareñas, J. L.; Alvarez-Puebla, R. A. *J. Am. Chem. Soc.* **2013**, *135*, 10314−10317.

(21) Wang, Y.; Yu, Z.; Ji, W.; Tanaka, Y.; Sui, H.; Zhao, B.; Ozaki, Y. *Angew. Chem., Int. Ed.* **2014**, *53*, 13866−13870.

(22) Ma, H.; Sun, X.; Chen, L.; Cheng, W.; Han, X. X.; Zhao, B.; He, C. *Anal. Chem.* **2017**, *89*, 8877−8883.

(23) Sun, F.; Galvan, D. D.; Jain, P.; Yu, Q. *Chem. Commun.* **2017**, *53*, 4550−4561.

(24) Kho, K. W.; Dinish, U. S.; Kumar, A.; Olivo, M. *ACS Nano* **2012**, *6*, 4892−4902.

(25) Tang, B.; Wang, J.; Hutchison, J. A.; Ma, L.; Zhang, N.; Guo, H.; Hu, Z.; Li, M.; Zhao, Y. *ACS Nano* **2016**, *10*, 871−879.

(26) Hodkiewicz, J.; Deck, F. *Evaluating Spectral Resolution on a Raman Spectrometer*, Thermo Fisher Scientific: Madison, WI, 2010.

(27) Chen, M.; Li, G.; Yan, J.; Lu, X.; Cui, J.; Ni, Z.; Cheng, W.; Qian, G.; Zhang, J.; Tu, H. *Clin. Chim. Acta* **2013**, *423*, 105.

(28) Šturcová, A.; Eichhorn, S. J.; Jarvis, M. C. *Biomacromolecules* **2006**, *7*, 2688−2691.

(29) Błasiak, B.; Londergan, C. H.; Webb, L. J.; Cho, M. *Acc. Chem. Res.* **2017**, *50*, 968−976.

(30) Capaldo, P.; Alfarano, S. R.; Ianeselli, L.; Zilio, S. D.; Bosco, A.; Parisse, P.; Casalis, L. *ACS Sens.* **2016**, *1*, 1003−1010.

(31) Liu, M.; Liu, G.-Y. *Langmuir* **2005**, *21*, 1972−1978.

(32) Dominguez, C. M.; Ramos, D.; Mendieta-Moreno, J. I.; Fierro, J. L. G.; Mendieta, J.; Tamayo, J.; Calleja, M. *Sci. Rep.* **2017**, *7*, 536.

(33) Gladney, A.; Qin, C.; Tamboue, H. *Open J. Phys. Chem.* **2012**, *2*, 117−122.

(34) Biselli, M.; Conti, F.; Gramenzi, A.; Frigerio, M.; Cucchetti, A.; Fatti, G.; D'Angelo, M.; Dall'Agata, M.; Giannini, E. G.; Farinati, F.; et al. *Br. J. Cancer* **2015**, *112*, 69−76.

(35) Karakatsanis, A.; Papaconstantinou, I.; Gazouli, M.; Lyberopoulou, A.; Polymeneas, G.; Voros, D. *Mol. Carcinog.* **2013**, *52*, 297−303.

(36) Yang, X.; Zhang, X.-F.; Lu, X.; Jia, H.-L.; Liang, L.; Dong, Q.-Z.; Ye, Q.-H.; Qin, L.-X. *Hepatology* **2014**, *59*, 1874−1885.

(37) Köberle, V.; Kronenberger, B.; Pleli, T.; Trojan, J.; Imelmann, E.; Peveling-Oberhag, J.; Welker, M.-W.; Elhendawy, M.; Zeuzem, S.; Piiper, A.; Waidmann, O. *Eur. J. Cancer* **2013**, *49*, 3442−3449.

DOI: 10.1021/acs.analchem.8b01798
Anal. Chem. 2018, 90, 10144−10151